Amorphous Aluminium Tunnel junctions

AlOx tunnel junctions

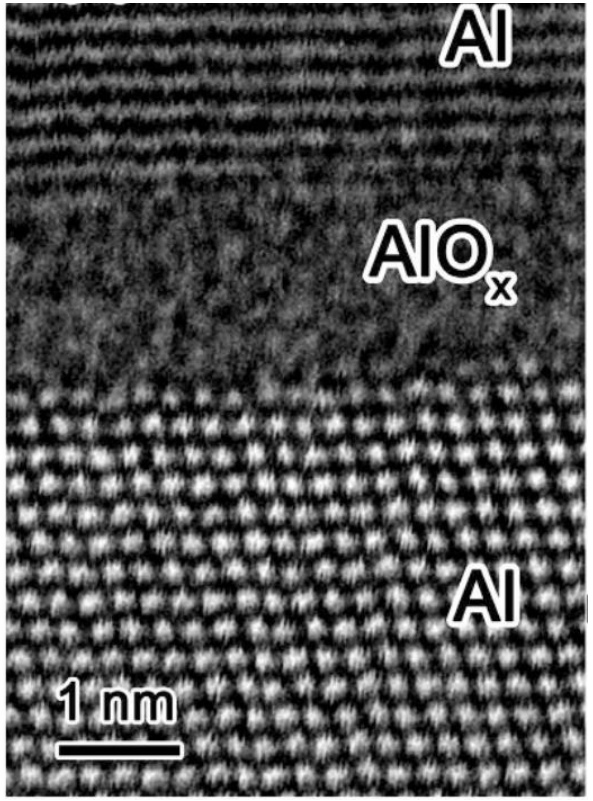

DOI: 10.1038/srep29679

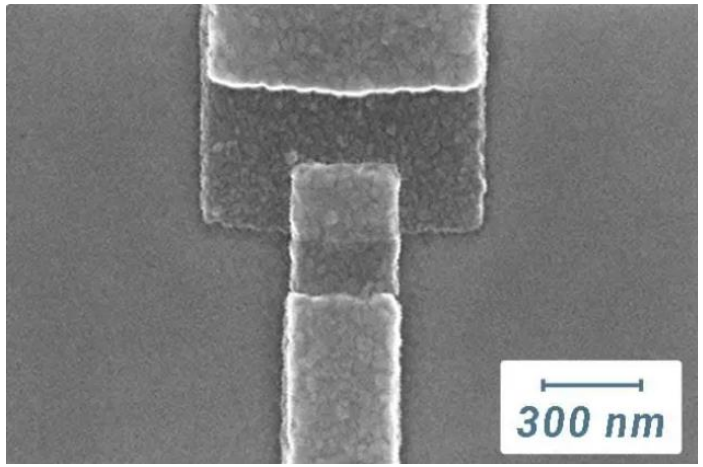

angstromengineering.com/

Superconducting devices:

- Josephson junctions→ SQUIDS, Transmon Qubits,..

Single-electronics **:**

- Single-Electron Transistors
- Coulomb blockade thermometers

Junction Fabrication:

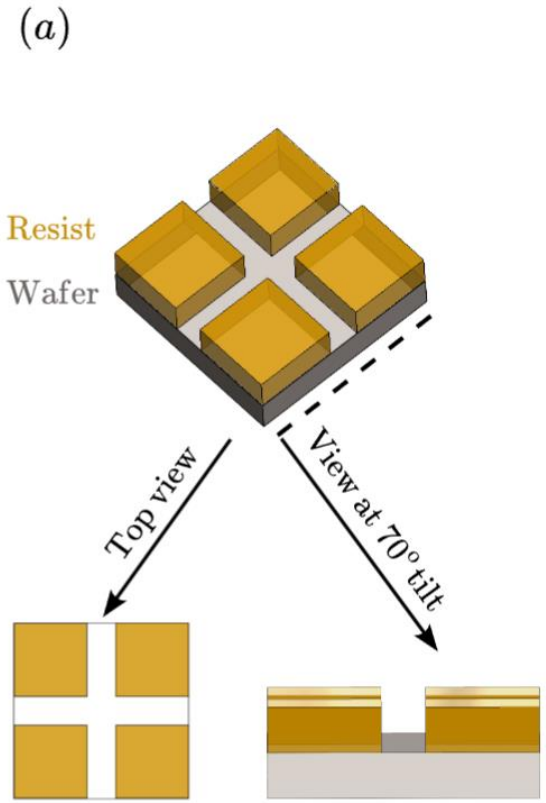

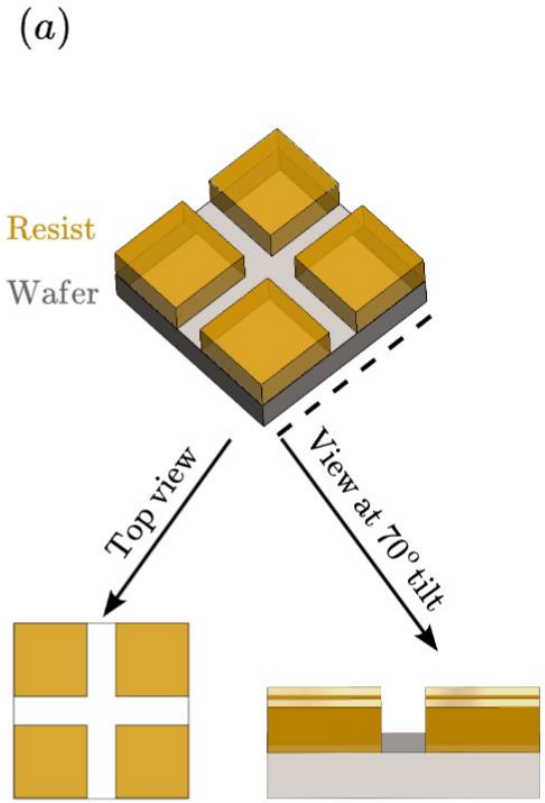
(a)
Resist
Wafer
Top view
View at 70° tilt

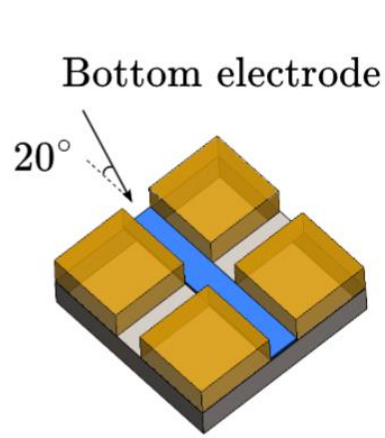
(b)
Bottom electrode
20°

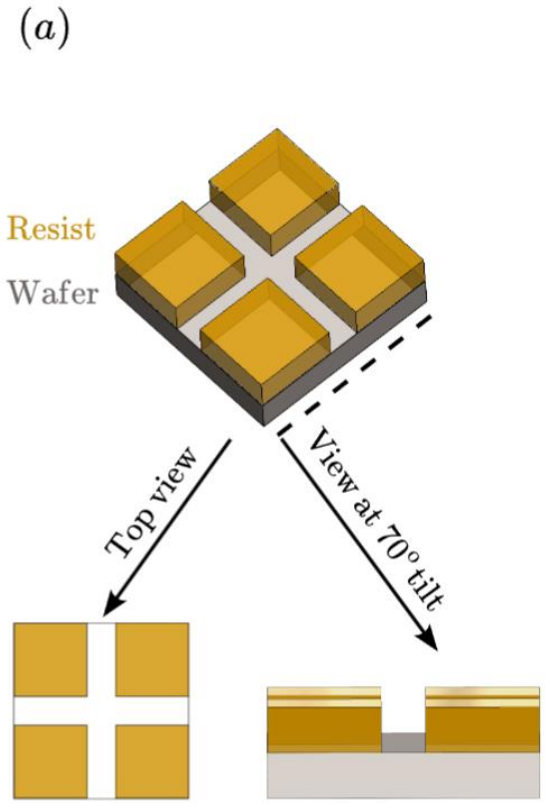
(a)
Resist
Wafer
Top view
View at 70° tilt

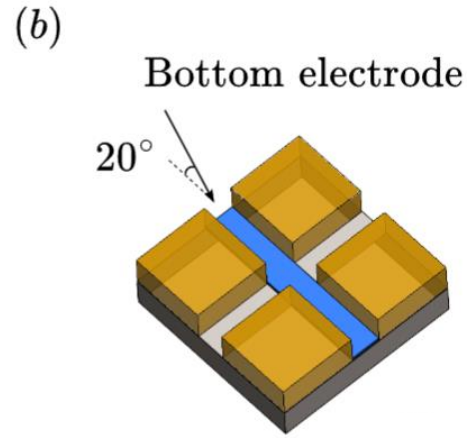
(b)
Bottom electrode
20°

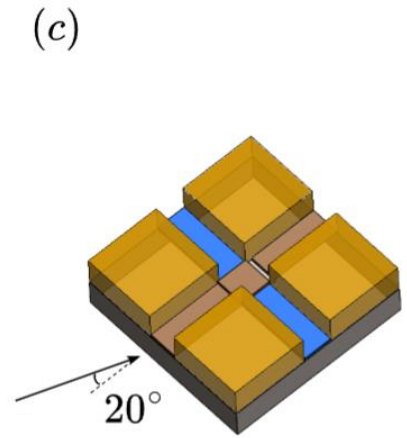
(c)
20°

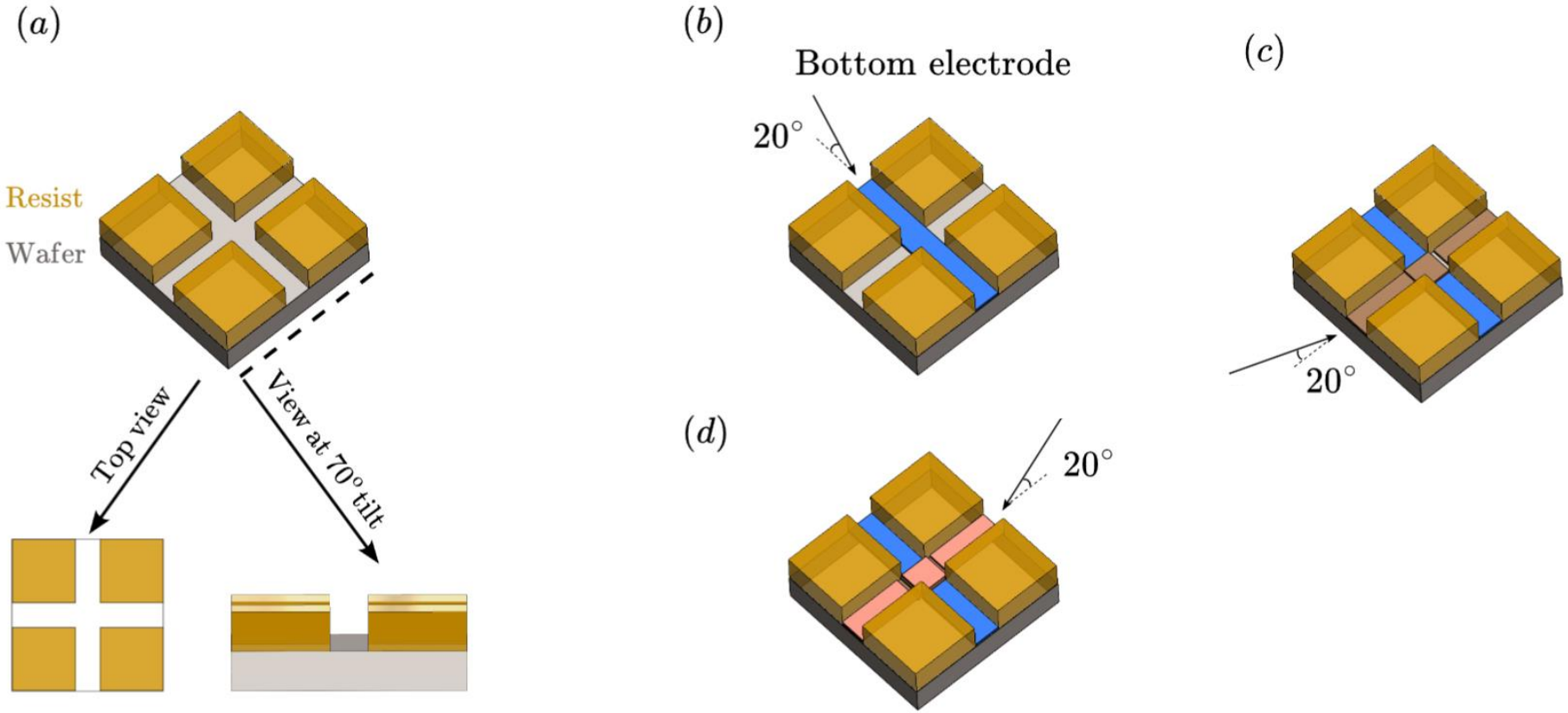
(a)
Resist
Wafer
Top view
View at 70° tilt
(b)
Bottom electrode
20°
(c)
20°
(d)
20°

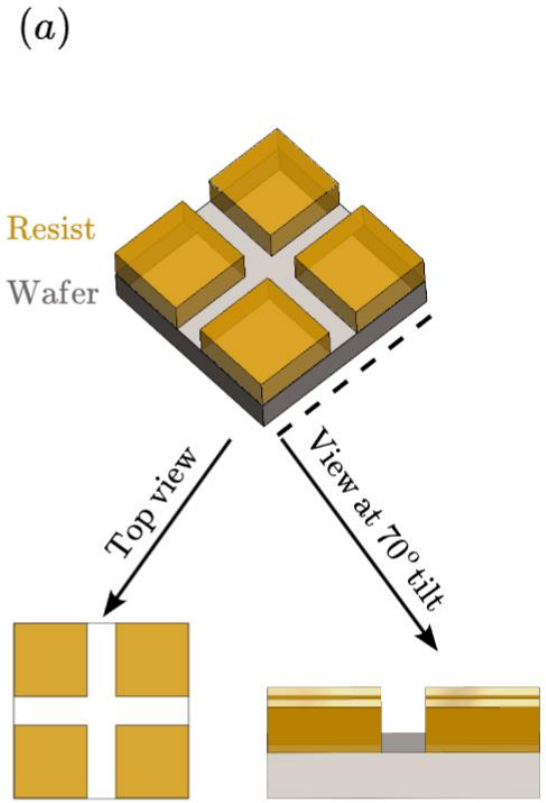
(a)
Resist
Wafer
Top view
View at 70° tilt

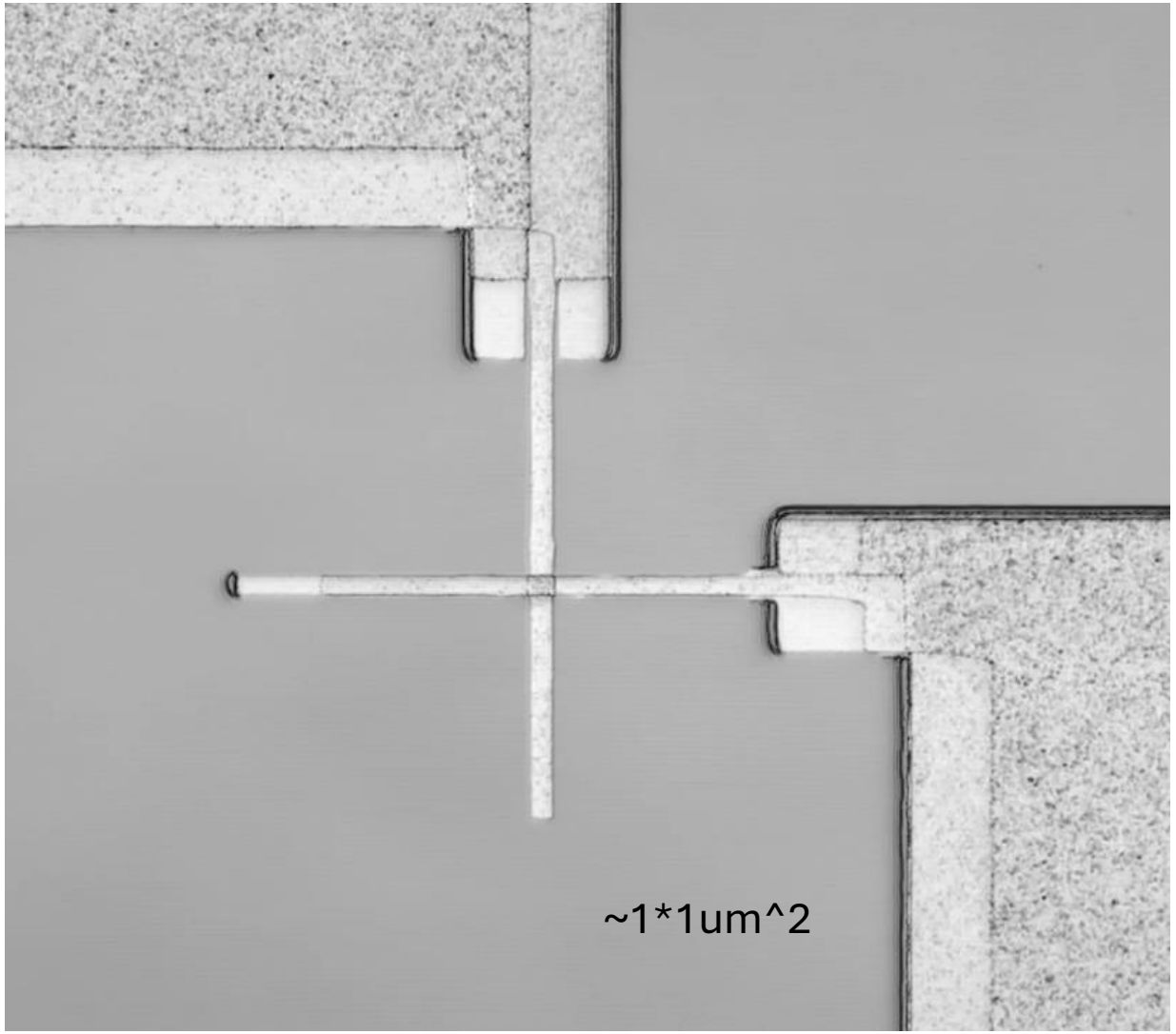
~1*1um^2

Problem: Amorphous

- Structural inhomogeneities
- Defects like TLS

Problem for SC qubits:

- Affect coherence and reproducibility, limiting scalability.

Problem in CBTs:

- Temperature dependent charging energy?

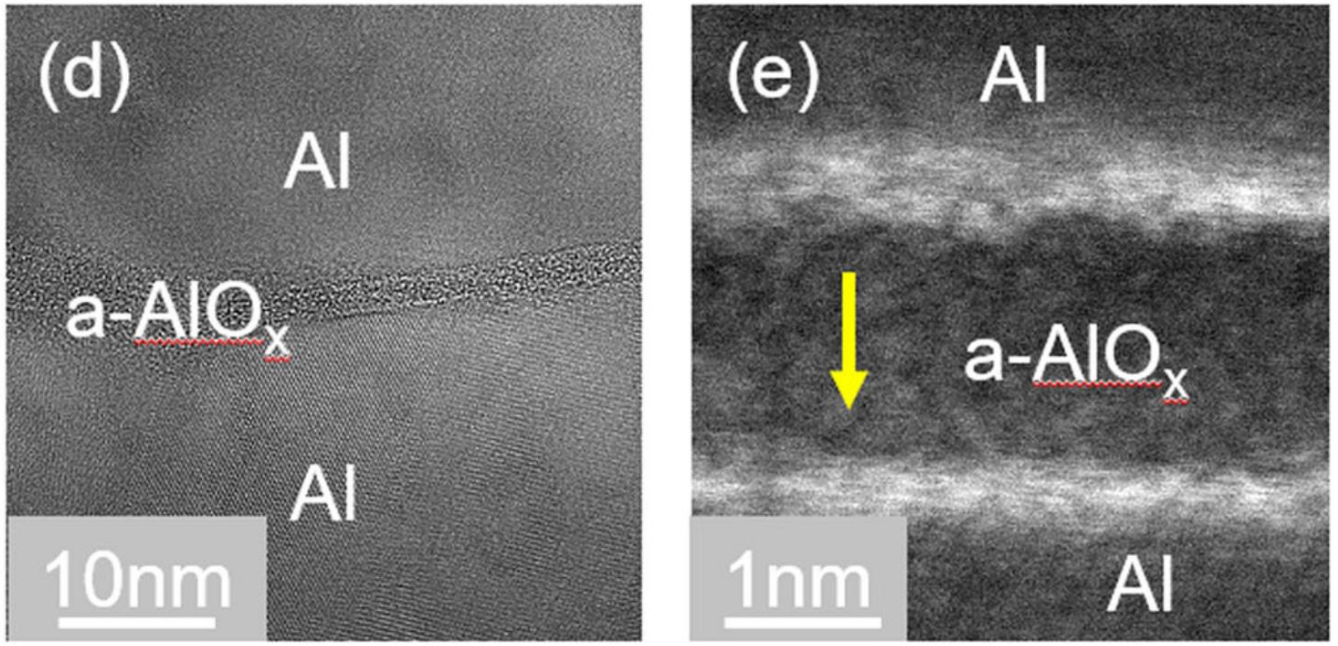

DOI: 10.1038/s43246-024-00596-z

ARTICLE OPEN

Check for updates

Simulating the fabrication of aluminium oxide tunnel junctions

M. J. Cyster[1], J. S. Smith[1], N. Vogt[1,2], G. Opletal[3], S. P. Russo[1] and J. H. Cole[1]✉

Aluminium oxide (AlO_x) tunnel junctions are important components in a range of nanoelectric devices including superconducting qubits where they can be used as Josephson junctions. While many improvements in the reproducibility and reliability of qubits have been made possible through new circuit designs, there are still knowledge gaps in the relevant materials science. A better understanding of how fabrication conditions affect the density, uniformity, and elemental composition of the oxide barrier may lead to the development of lower noise and more reliable nanoelectronics and quantum computers. In this paper, we use molecular dynamics to develop models of Al–AlO_x–Al junctions by iteratively growing the structures with sequential calculations. With this approach, we can see how the surface oxide grows and changes during the oxidation simulation. Dynamic processes such as the evolution of a charge gradient across the oxide, the formation of holes in the oxide layer, and changes between amorphous and semi-crystalline phases are observed. Our results are widely in agreement with previous work including reported oxide densities, self-limiting of the oxidation, and increased crystallinity as the simulation temperature is raised. The encapsulation of the oxide with metal evaporation is also studied atom by atom. Low density regions at the metal–oxide interfaces are a common feature in the final junction structures which persists for different oxidation parameters, empirical potentials, and crystal orientations of the aluminium substrate.

npj Quantum Information (2021)7:12 ; https://doi.org/10.1038/s41534-020-00360-4

Oxidation

Top View

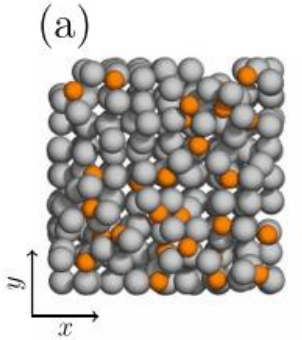

Side View

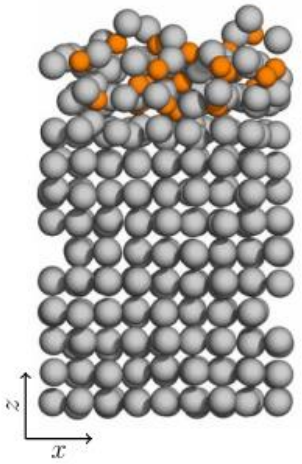

30 oxygen atoms

16 × 16 Å^2 on Al(100) surface

Oxidation

Top View

Side View

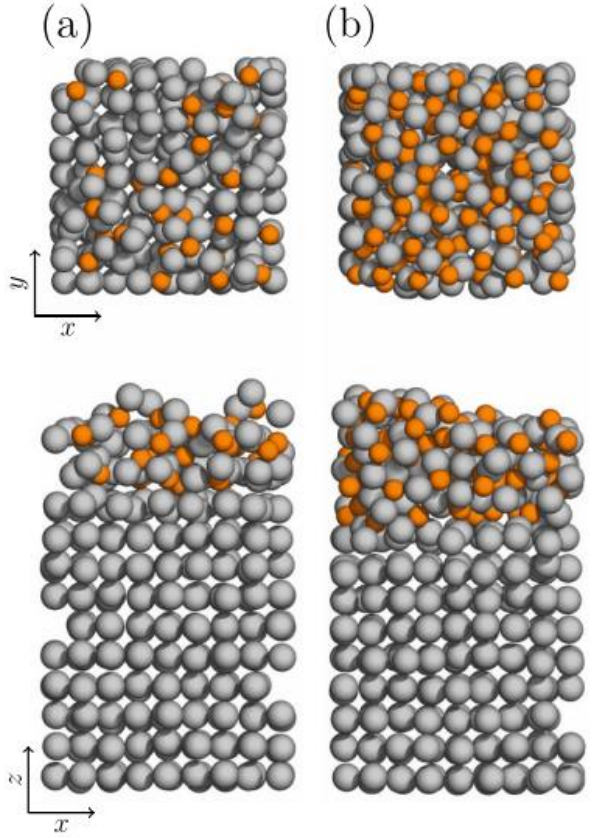

90 oxygen atoms

Oxidation

Top View

Side View

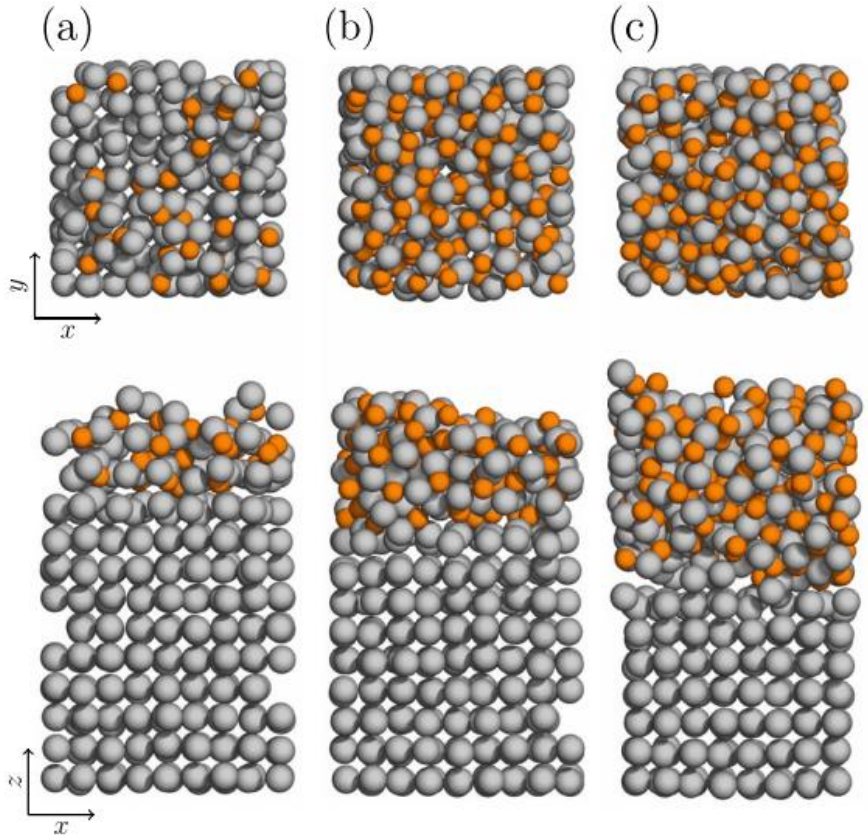

150 oxygen atoms

Metallization

(d)

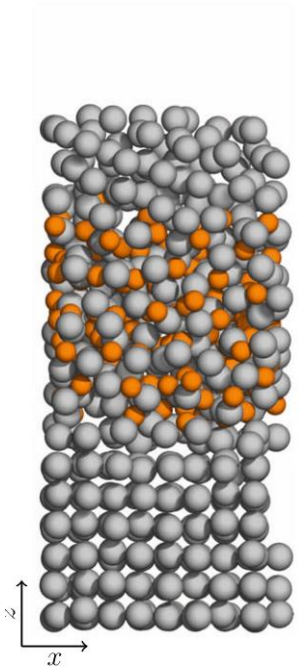

Metallization

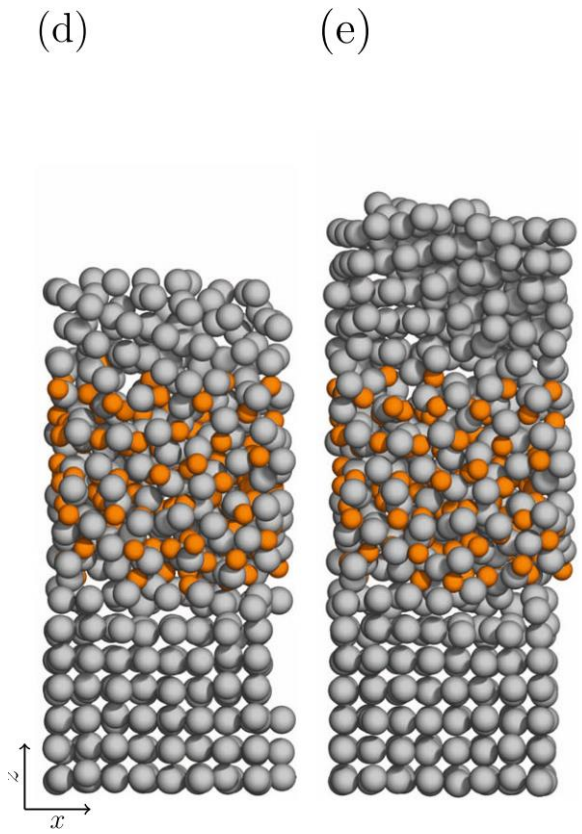

Metallization

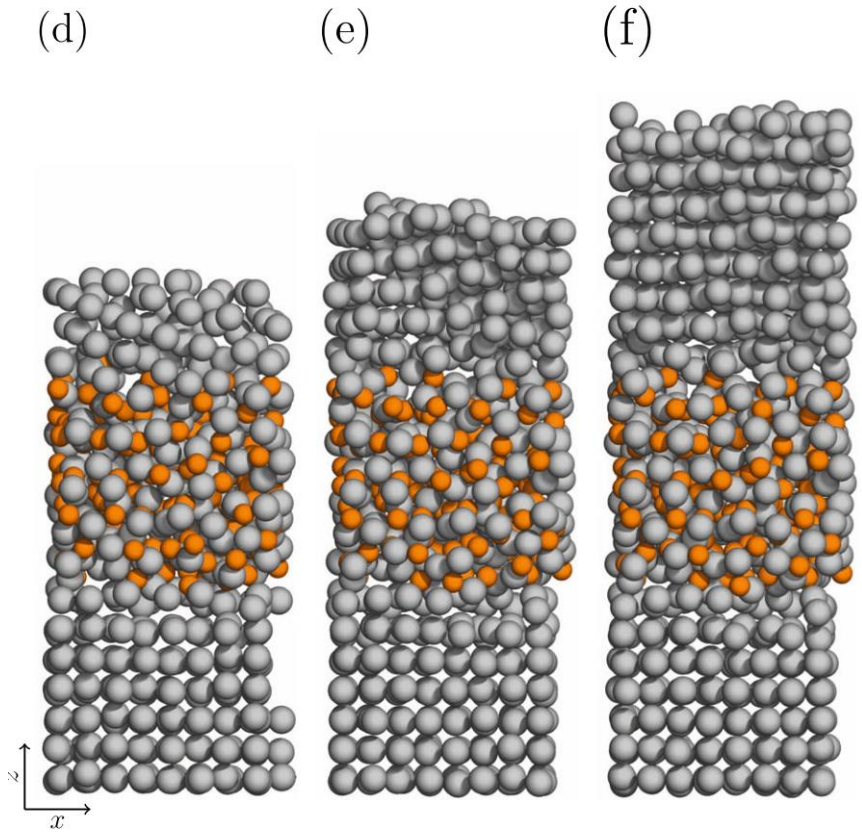

Metallization

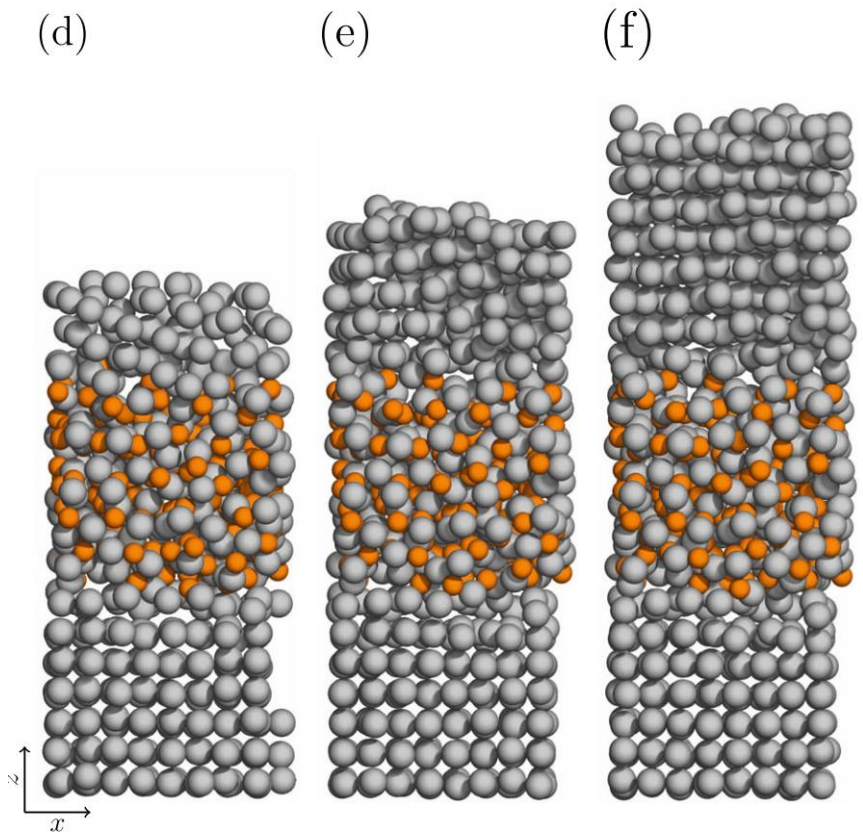

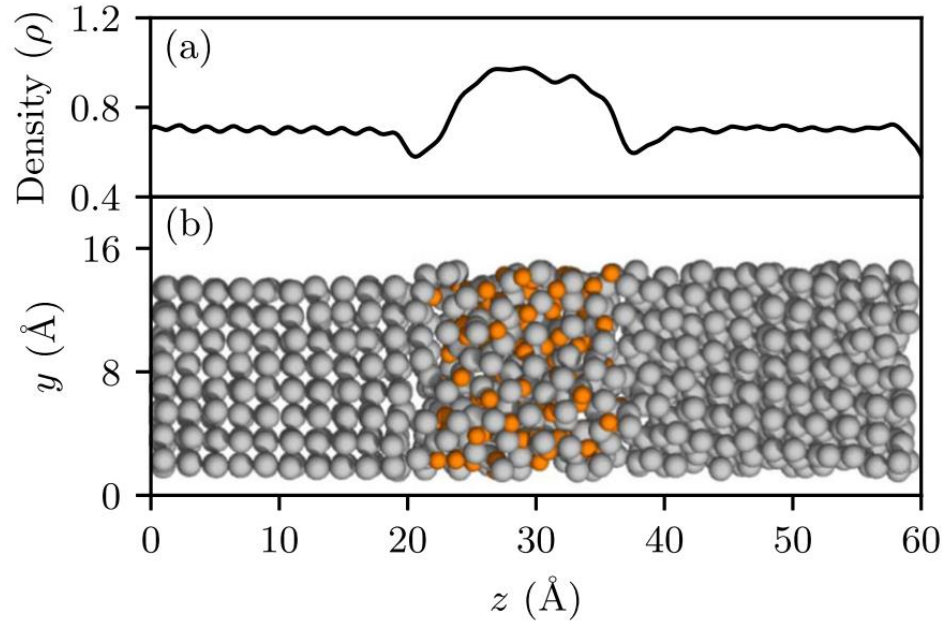

Fig. 2 Density analysis of a junction model. a The material density in the junction model as a function of position. **b** The final atomic structure of a Al–AlO_x–Al junction model where oxygen and aluminium atoms are depicted as orange and grey spheres, respectively. This calculation was performed with the S–M potential.

Diminishing Crystallinity

a single O atom can diminish the Crytal structure

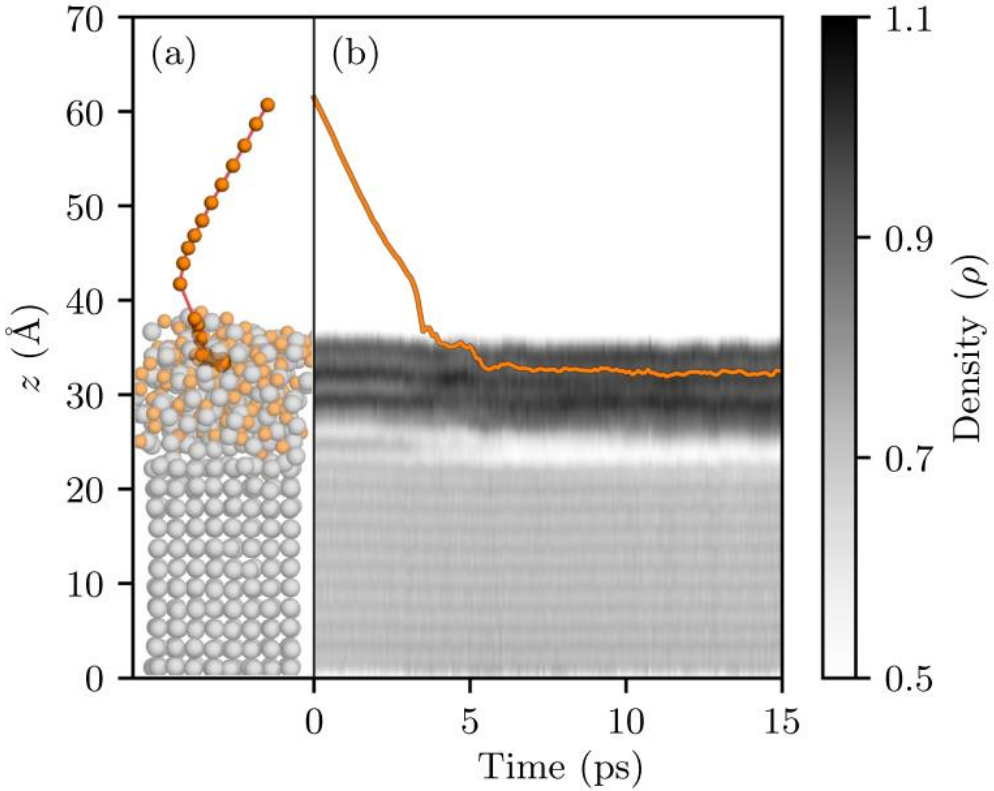

Diminishing Crystallinity

a single O atom can diminish the Crytal structure

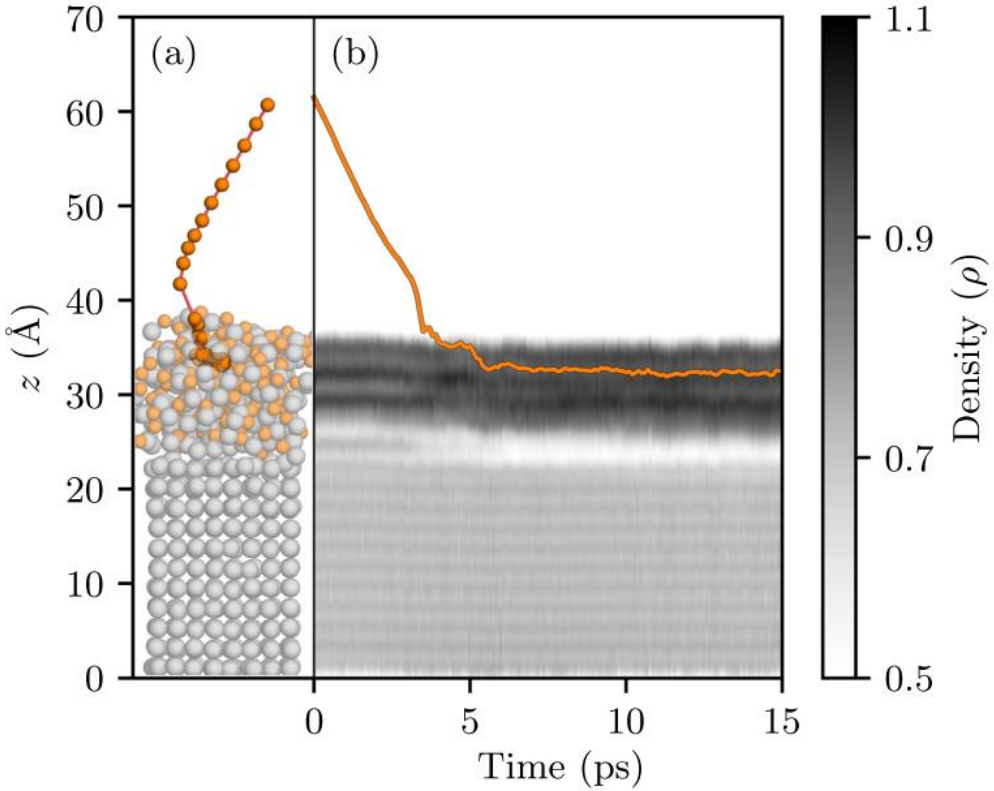

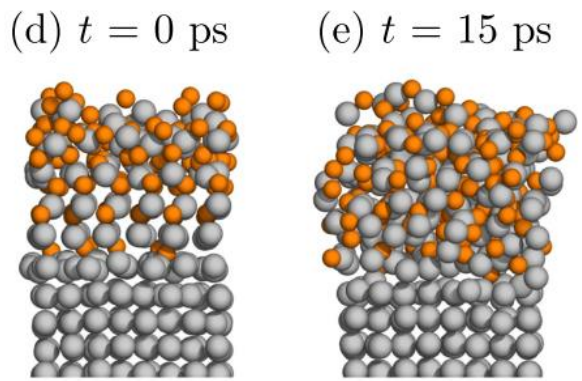

Structural properties during the oxidation simulation

- AlOx/vacuum interface is oxygen rich compared with the Al/AlOx interface
- Oxide growth is limited in crystal phase?

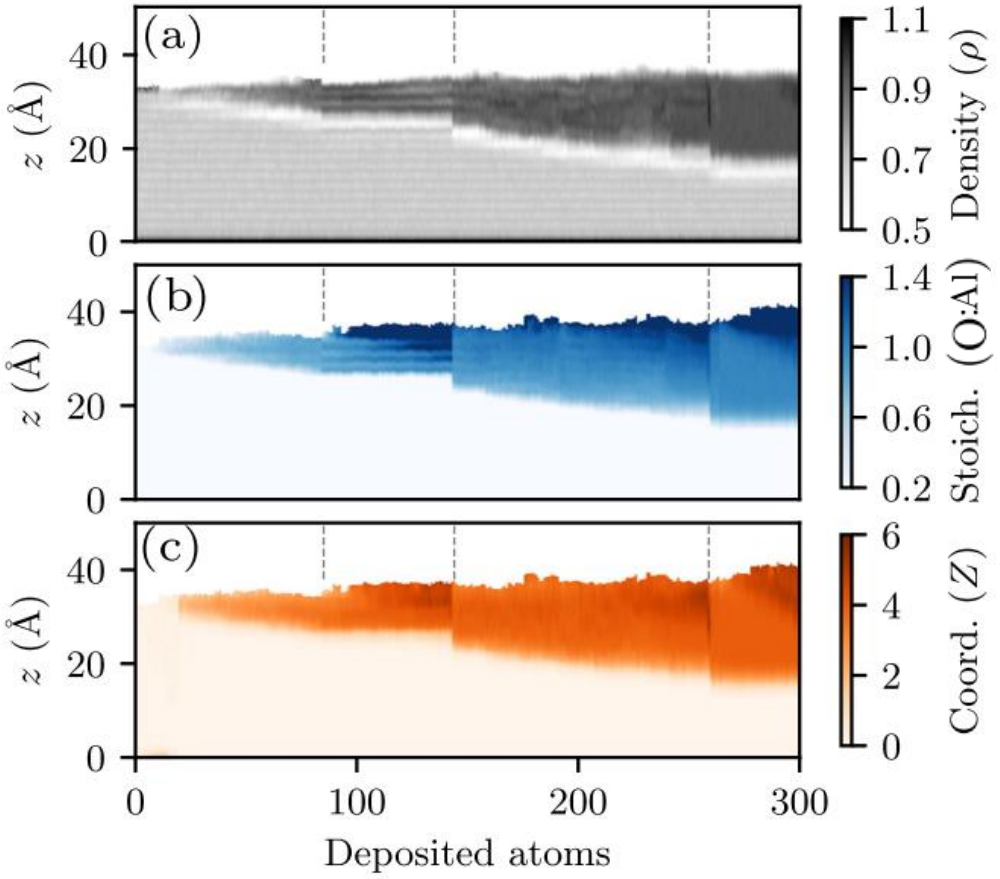

Effect of Temperature on Oxidation

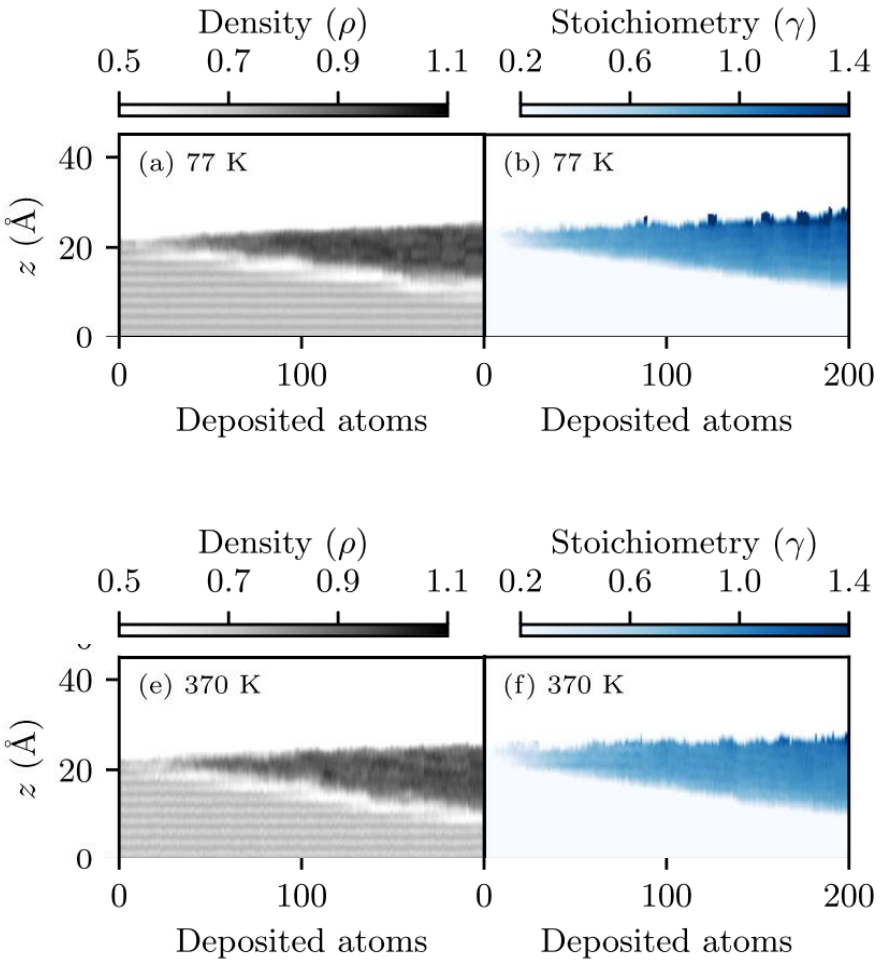

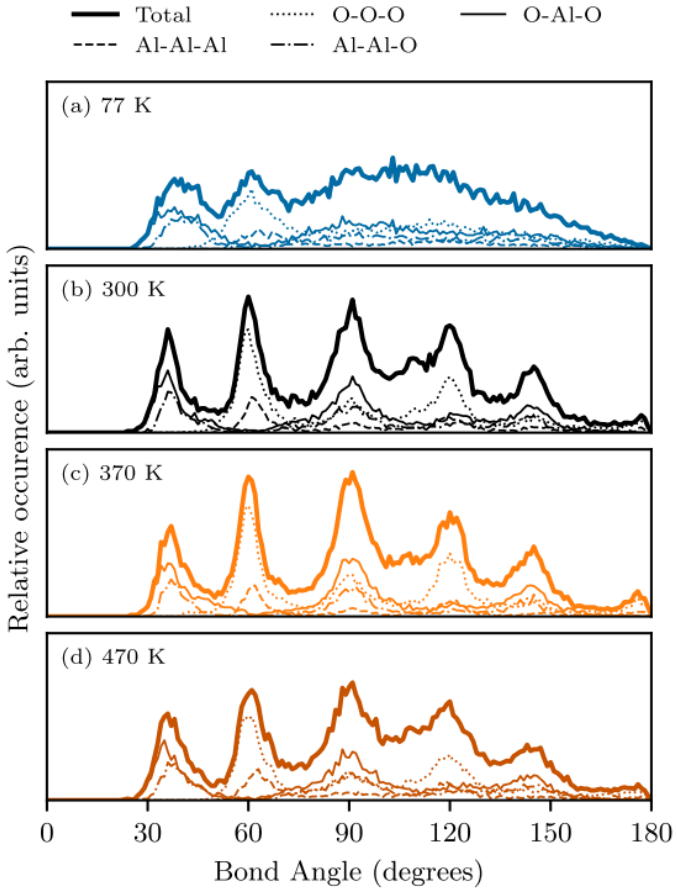

Fig. 6 The effect of temperature on the bond angles in the completed oxide structures. Bond angles in the surface oxide following simulated oxidation at temperatures of (**a**) 77, (**b**) 300, (**c**) 370, and (**d**) 470 K.

Top electrode

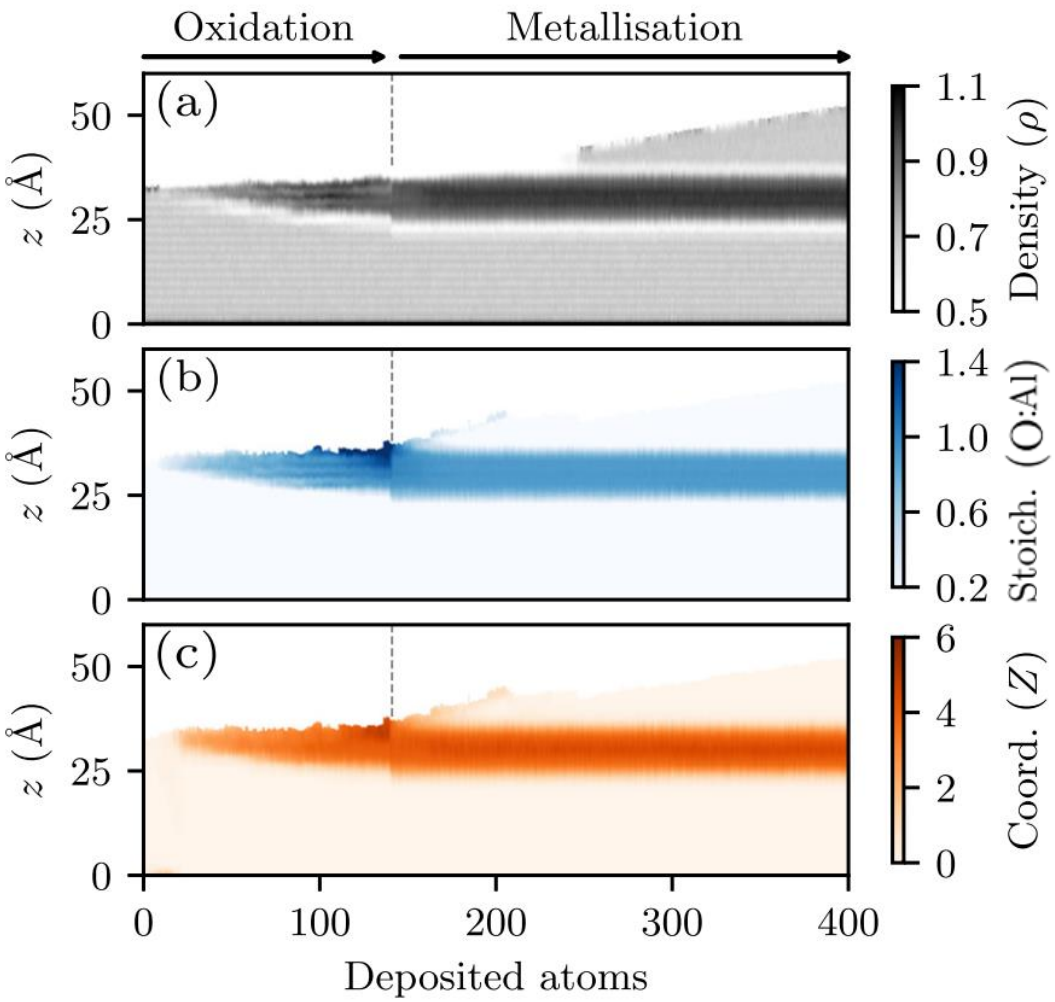

Partial charges in the structure at various stages

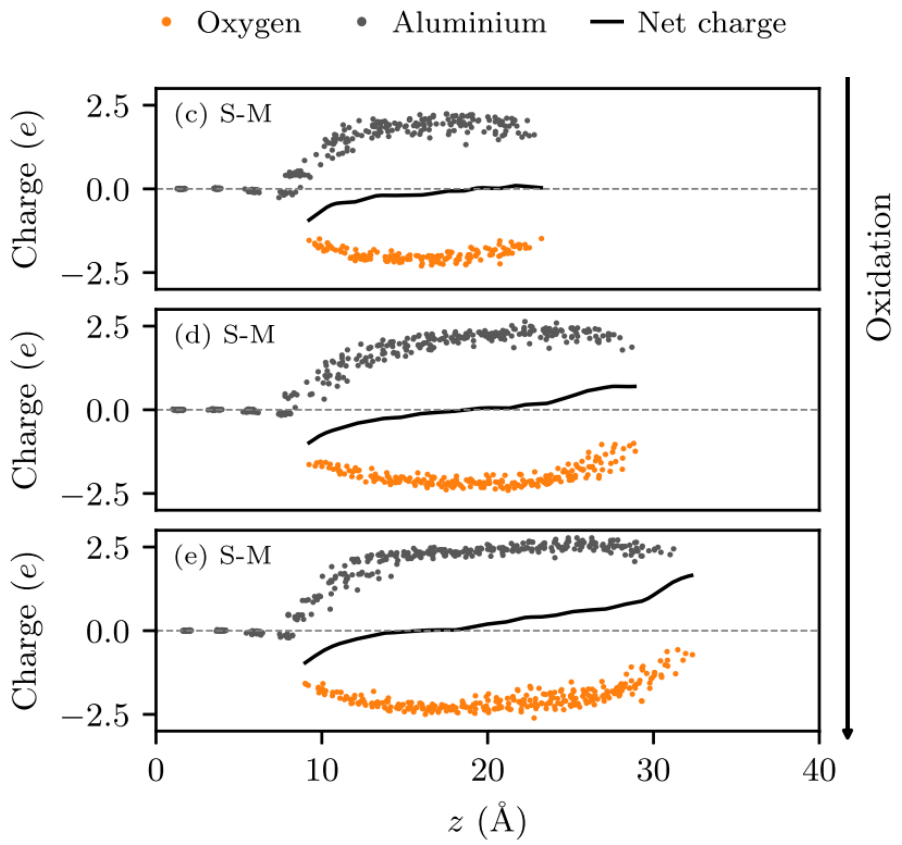

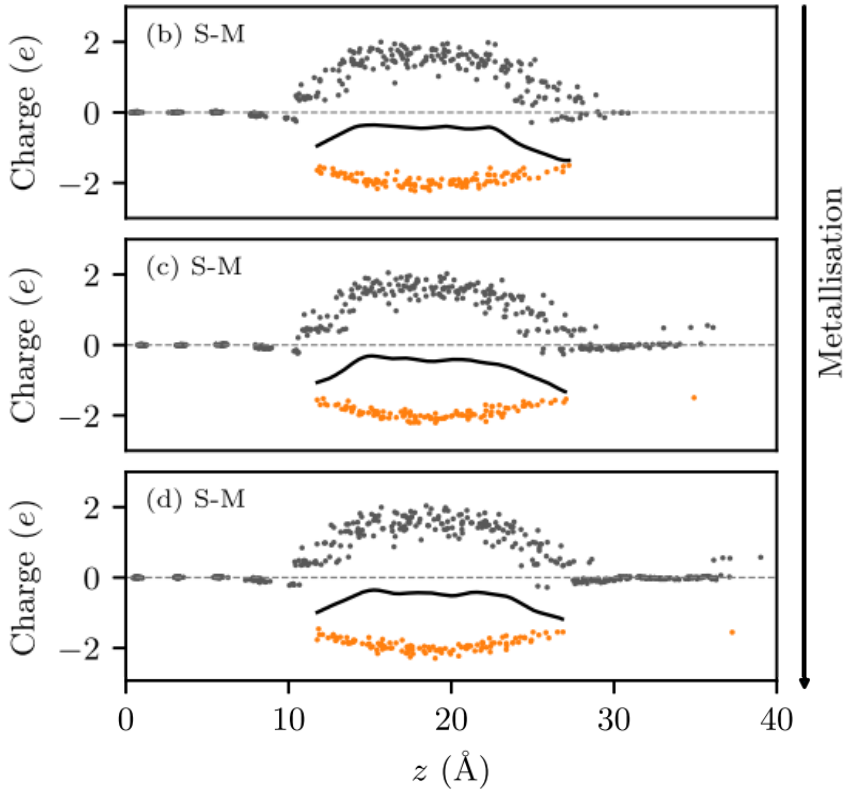

SCIENTIFIC REPORTS

OPEN

Correlating the nanostructure of Al-oxide with deposition conditions and dielectric contributions of two-level systems in perspective of superconducting quantum circuits

Received: 4 December 2017
Accepted: 4 May 2018
Published online: 21 May 2018

S. Fritz[1], A. Seiler[2], L. Radtke[2], R. Schneider[1], M. Weides[2,3], G. Weiß[2] & D. Gerthsen[1]

Samples

•**EBPlas**: Electron-beam deposition with dynamic oxidation.

•**EBPlas-UV**: Same as EBPlas, but with UV illumination during oxidation.

•**EBLes**: Electron-beam deposition using Al_2O_3 pellets.
in *PVD 75, Kurt J. Lesker Company, Hastings, UK*

•**SPUT**: Sputter deposition with an Ar/O plasma mixture

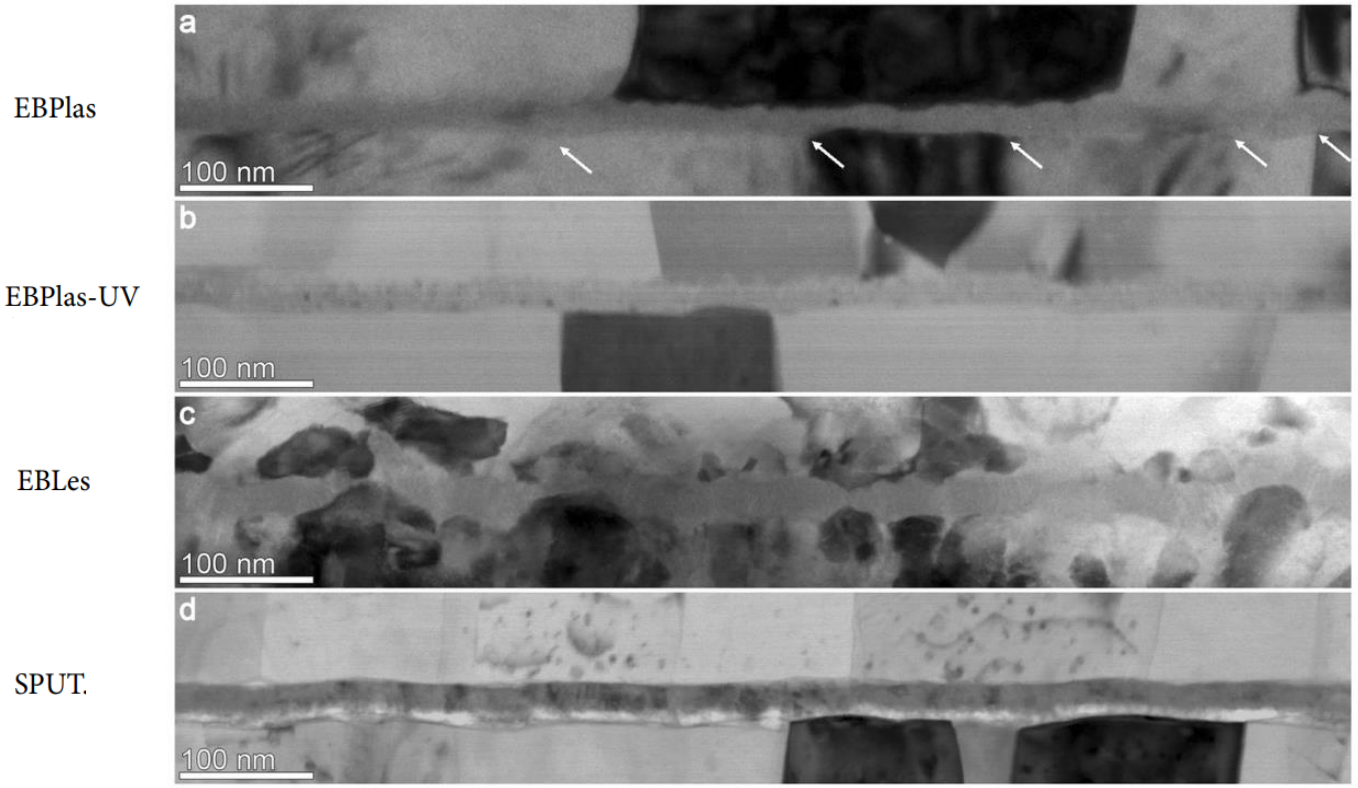

- 20-30 nm thick oxide- repetitive E&O

High-Res cross-section TEM

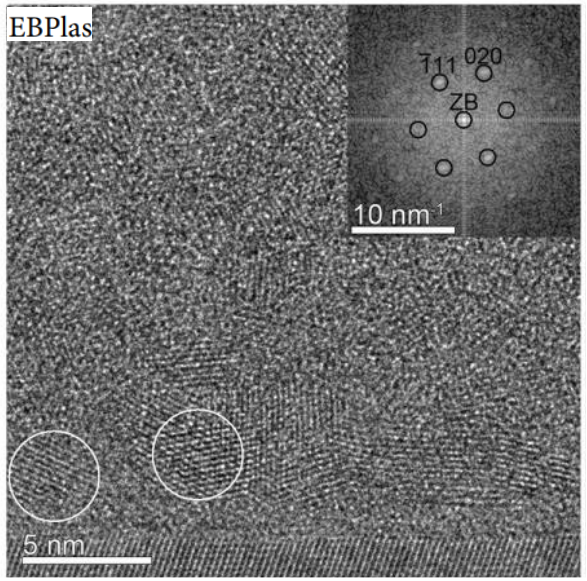

FT pattern of an Al-nanocrystal in [110] zone-axis

High-Res cross-section TEM

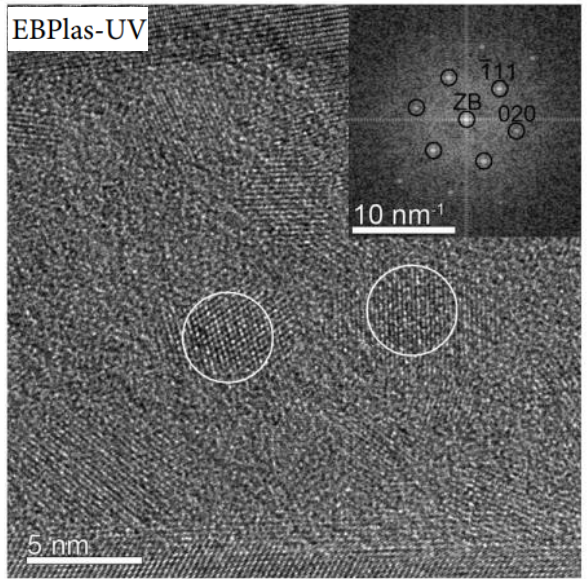

FT pattern of an Al-nanocrystal in [110] zone-axis

High-Res cross-section TEM

FT pattern of γ-Al_2O_3 in the [101] zone-axis

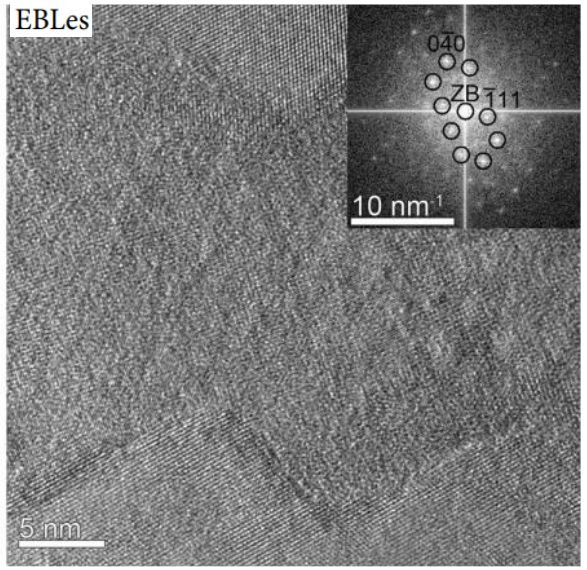

High-Res cross-section TEM

FT pattern of γ-Al_2O_3 in the [103] zone-axis

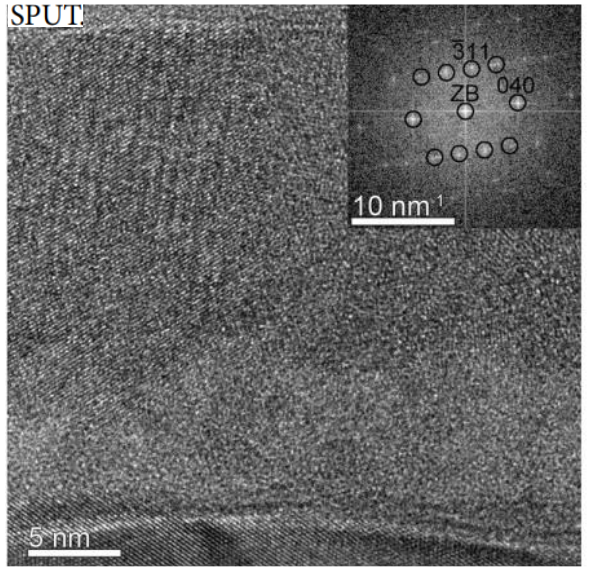

EELS spectra

Al-$L_{2,3}$ O-K

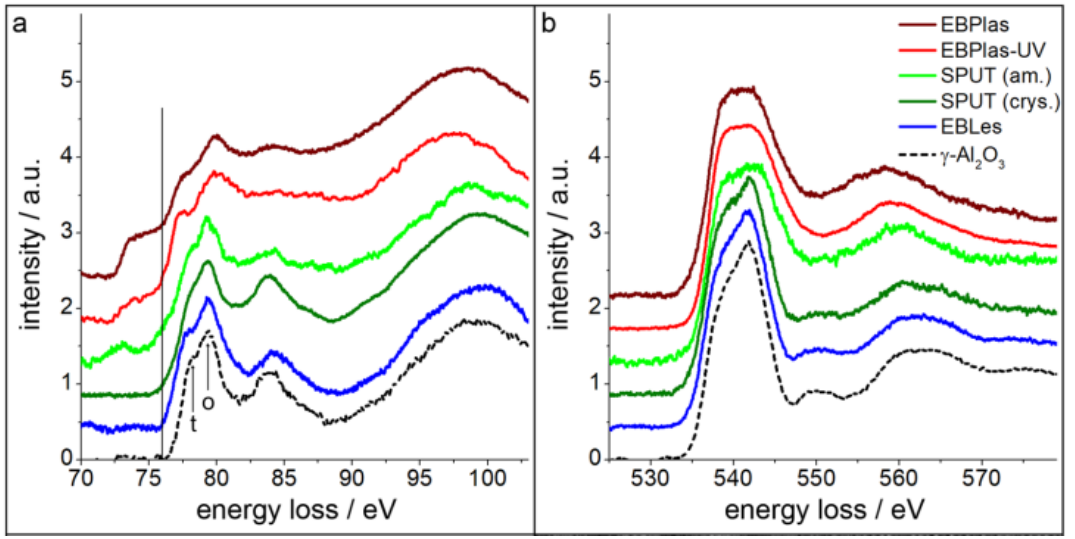

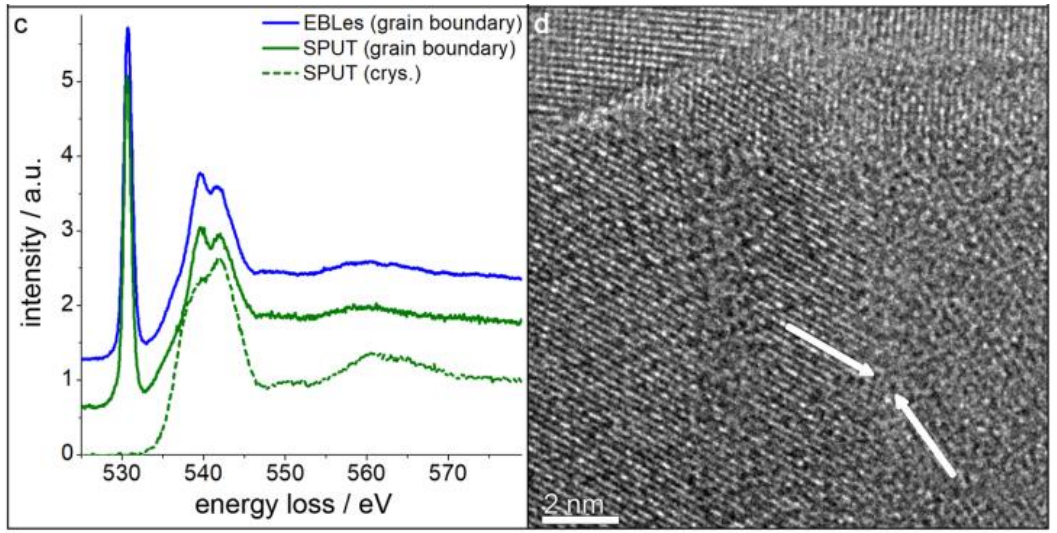

Chemical composition of different regions

sample	region	chemical composition AlO_x
EBPlas	amorphous	0.48 ± 0.04
	crystalline	Al
EBPlas-UV	amorphous	1.10 ± 0.06
	crystalline	Al
EBLes	amorphous	1.31 ± 0.03
	crystalline	1.50 ± 0.04
	grain boundaries	1.73 ± 0.10
SPUT	amorphous	1.18 ± 0.05
	crystalline	1.49 ± 0.03
	grain boundaries	1.82 ± 0.10

Capacitance measurements

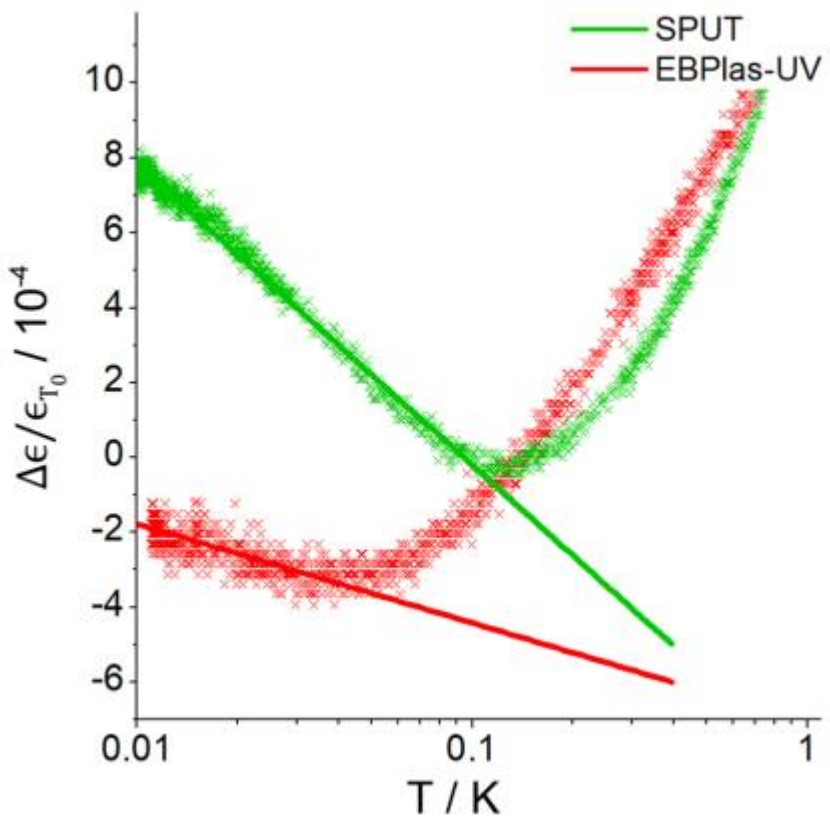

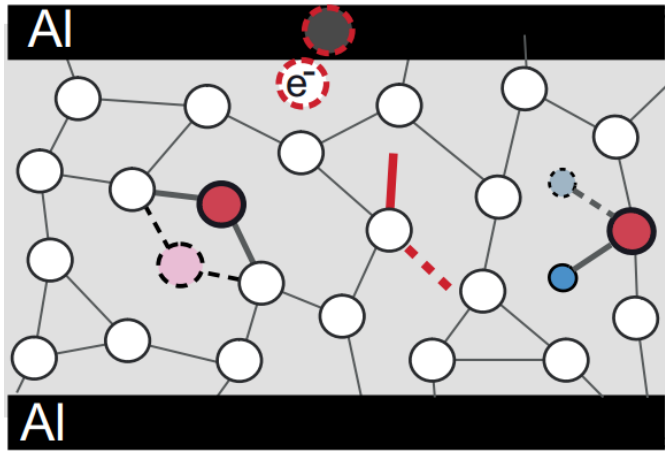

DOI: 10.1038/srep23786

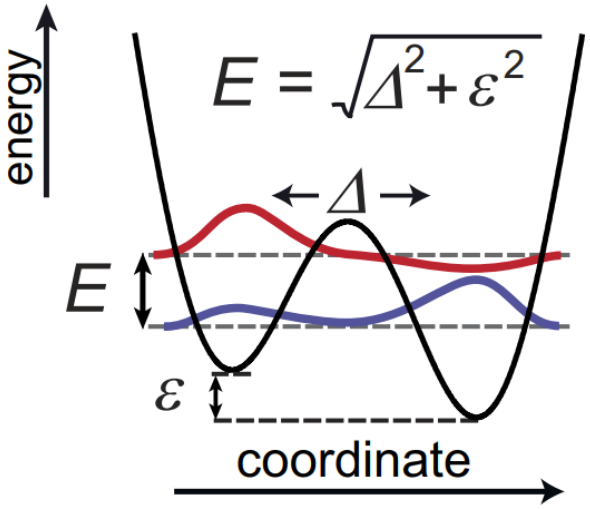

$$\chi_{TLS}(T) = \kappa \cdot \log\left(\frac{T_0}{T}\right)$$

$$\kappa \propto N \cdot p^2$$

$$\Delta C/C_{T_0} = \Delta\epsilon/\epsilon_{T_0} = \Delta\chi_{\mathrm{TLS}}/\epsilon_{T_0}$$

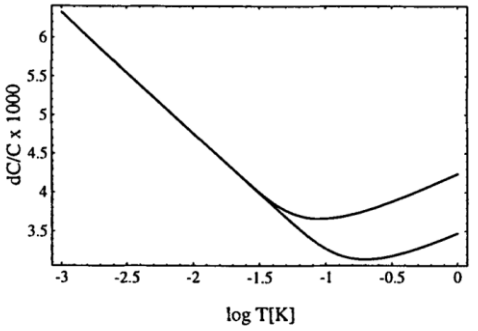

Figure 1: Calculated dielectric response, $\epsilon'(\omega)$, for BK7 vs. $\log(T)$ showing the frequency dependence above T_{min}. For the upper curve $\omega/2\pi = 500Hz$ was used, and for the lower curve $\omega/2\pi = 5kHz$.

10.1007/BF02548143

Capacitance measurements

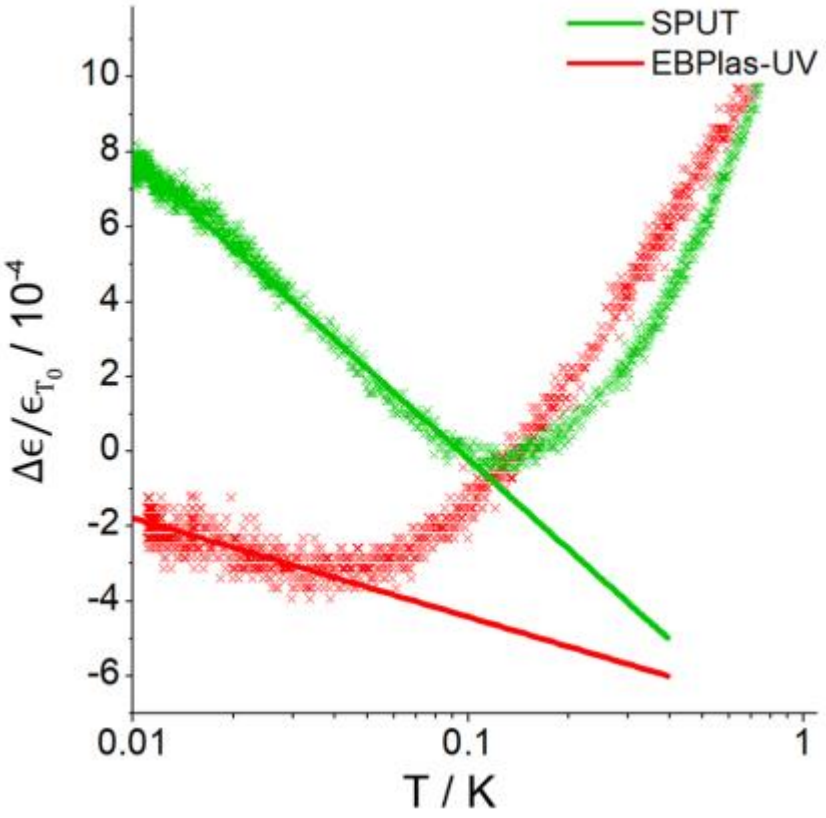

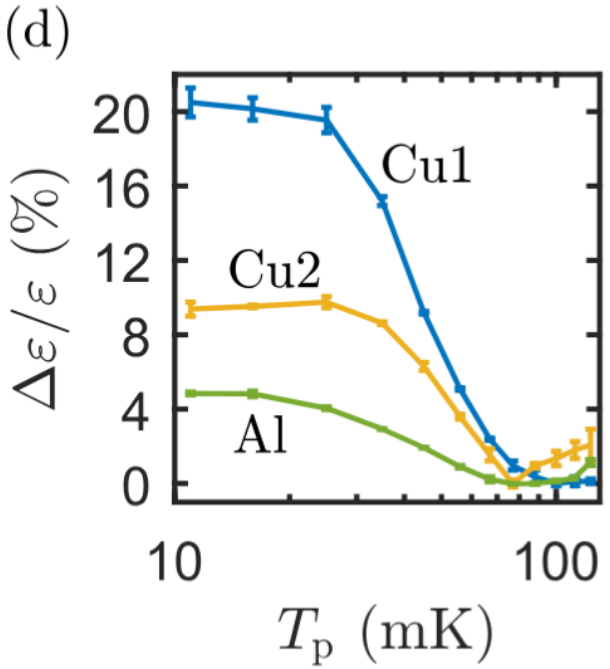

In SPUT:
loosely bound O_2 at grain boundaries in γ-Al_2O_3 layer → weakly coupled TLS to phonons, increasing ϵ.

communications materials

Article

https://doi.org/10.1038/s43246-024-00596-z

Alternating-bias assisted annealing of amorphous oxide tunnel junctions

Check for updates

David P. Pappas[1,4] ✉, Mark Field[1,4], Cameron J. Kopas[1,4], Joel A. Howard[1,4], Xiqiao Wang[1,4], Ella Lachman[1], Jinsu Oh[2], Lin Zhou[2,3,4], Alysson Gold[1], Gregory M. Stiehl[1], Kameshwar Yadavalli[1,5], Eyob A. Sete[1], Andrew Bestwick[1,5], Matthew J. Kramer[2,3,5] & Josh Y. Mutus[1,5] ✉

Superconducting quantum bits (qubits) rely on ultra-thin, amorphous oxide tunneling barriers that can have significant inhomogeneities and defects as grown. This can result in relatively large uncertainties and deleterious effects in the circuits, limiting the scalability. Finding a robust solution to the junction reproducibility problem has been a long-standing goal in the field. Here, we demonstrate a transformational technique for controllably tuning the electrical properties of aluminum-oxide tunnel junctions. This is accomplished using a low-voltage, alternating-bias applied individually to the tunnel junctions, with which resistance tuning by more than 70% can be achieved. The data indicates an improvement of coherence and reduction of two-level system defects. Transmission electron microscopy shows that the treated junctions are predominantly amorphous, albeit with a more uniform distribution of alumina coordination across the barrier. This technique is expected to be useful for other devices based on ionic amorphous materials.

Cabrera-Mott Model:
•Aluminum/oxygen kinetics driven by intrinsic electric field.
•Self-limiting oxide growth.

Oxide Formation:
Driven by strong electric field (~1 GV/m).

Mott Voltage:
For Al_2O_3: V_Mott ≈ 0.5–1 V.

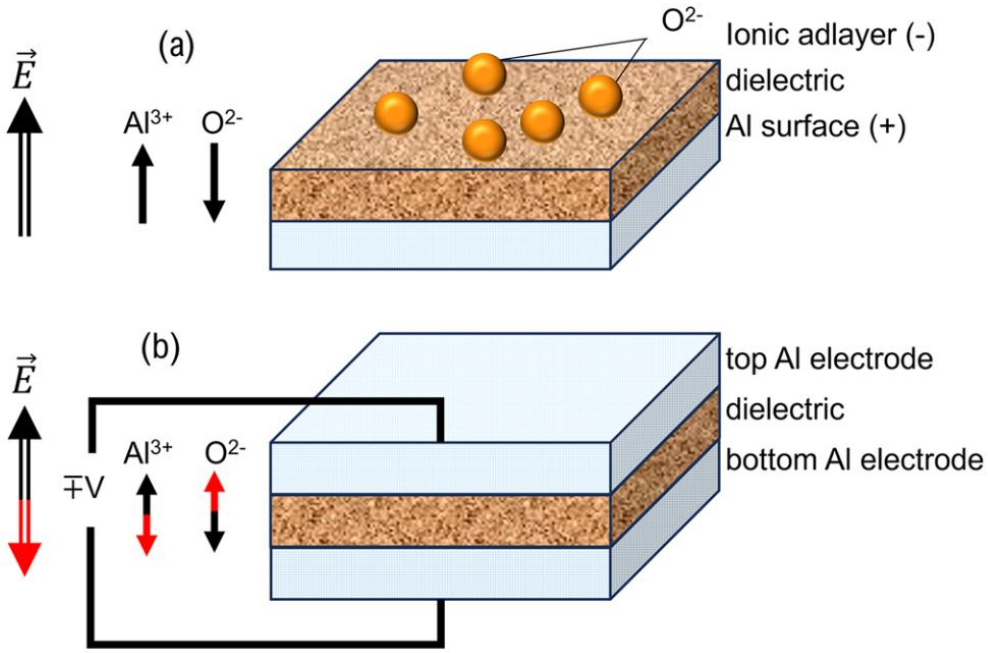

ABAA method

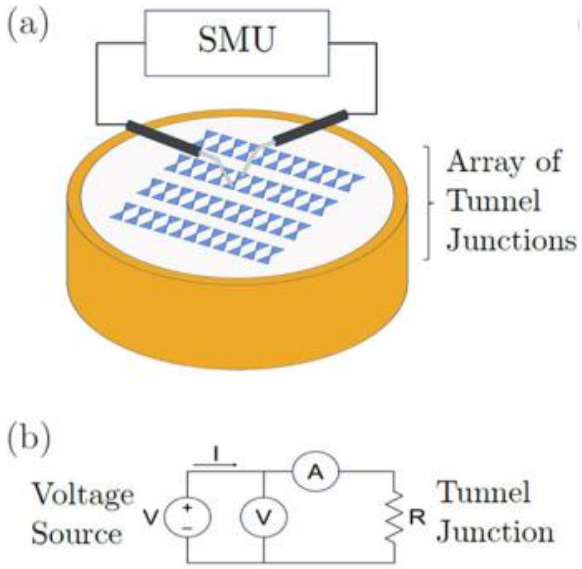
(a)
SMU
Array of
Tunnel
Junctions
(b)
I
A
Voltage
Source
V
+
−
V
R
Tunnel
Junction

ABAA method

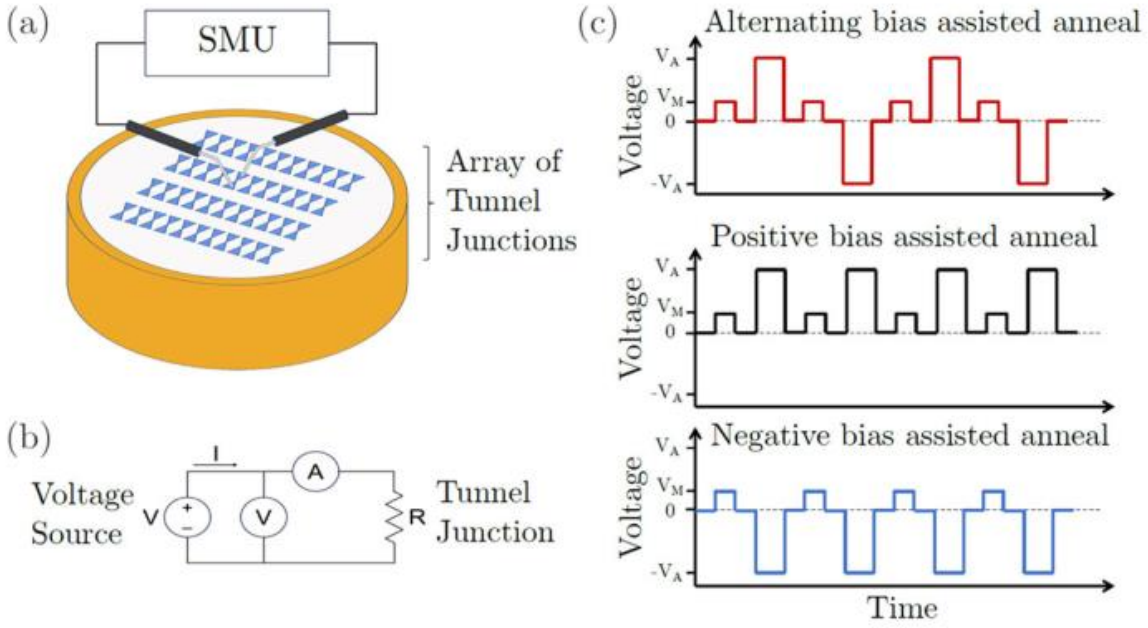
(a)
SMU
Array of
Tunnel
Junctions
(b)
I
A
Voltage
Source
V
+
−
V
R
Tunnel
Junction
(c)
Alternating bias assisted anneal
Positive bias assisted anneal
Negative bias assisted anneal
Voltage
V_A
V_M
0
$-V_A$
Time

ABAA method

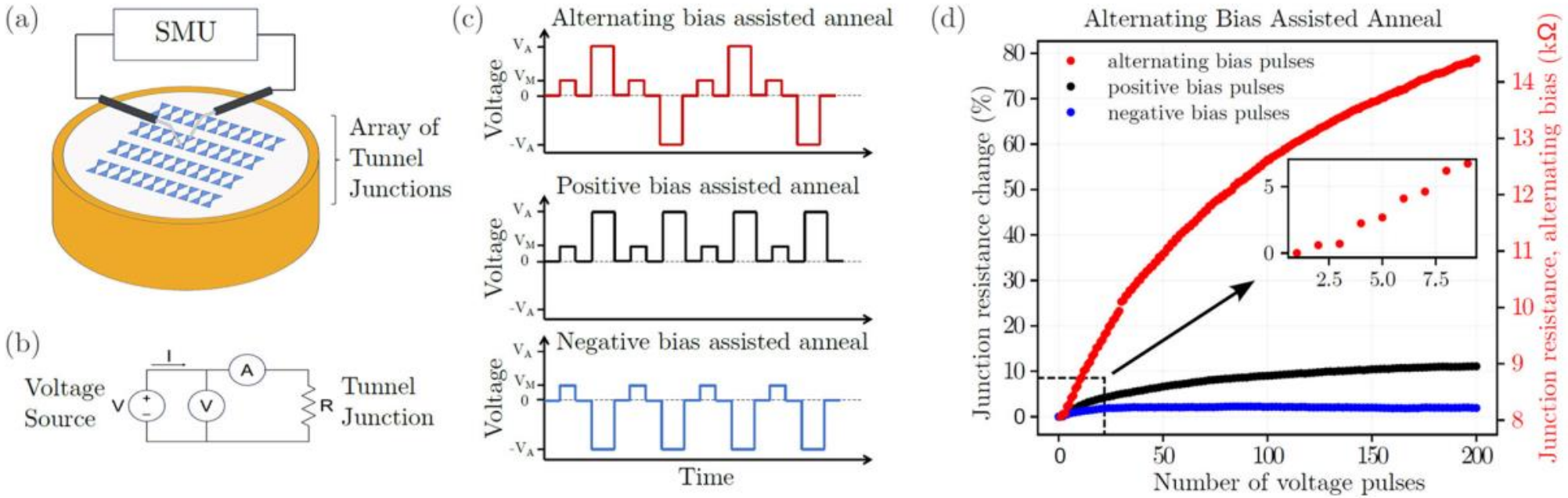
(a)
SMU
Array of
Tunnel
Junctions
(b)
I
A
Voltage
Source
V
R
Tunnel
Junction
(c)
Alternating bias assisted anneal
Positive bias assisted anneal
Negative bias assisted anneal
Voltage
Time
(d)
Alternating Bias Assisted Anneal
alternating bias pulses
positive bias pulses
negative bias pulses
Junction resistance change (%)
Junction resistance, alternating bias (kΩ)
Number of voltage pulses

Effect of Temperature

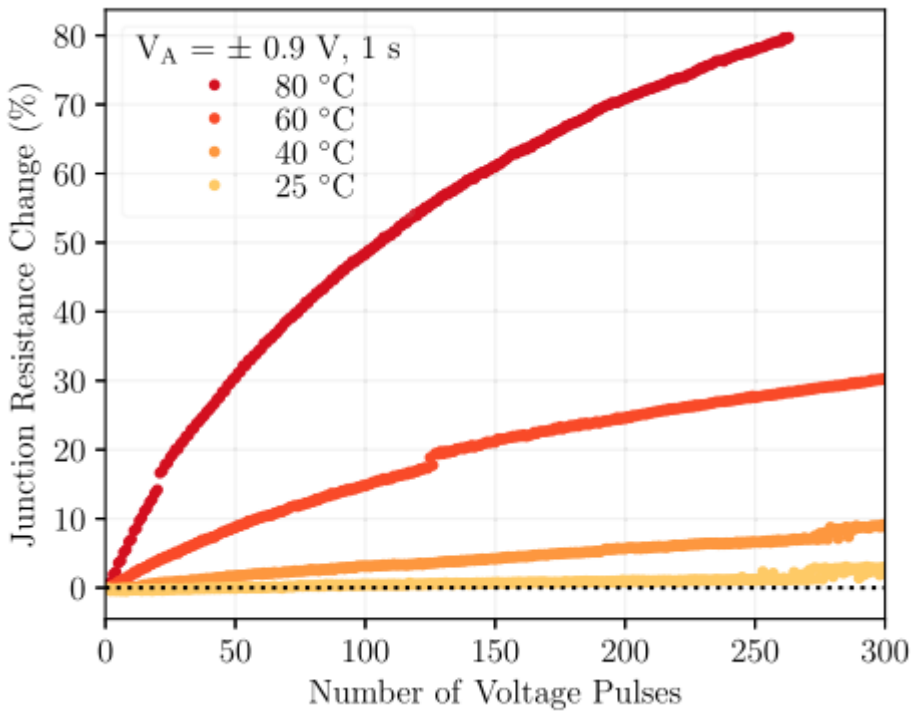

Still Amorphous

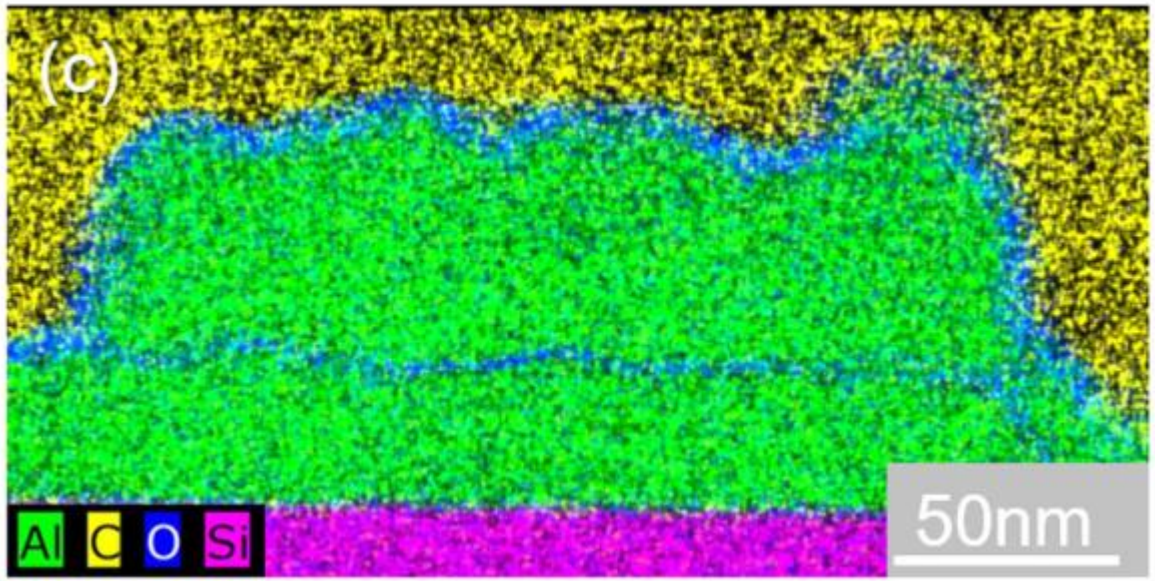

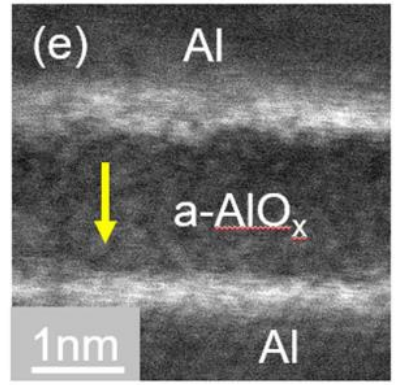

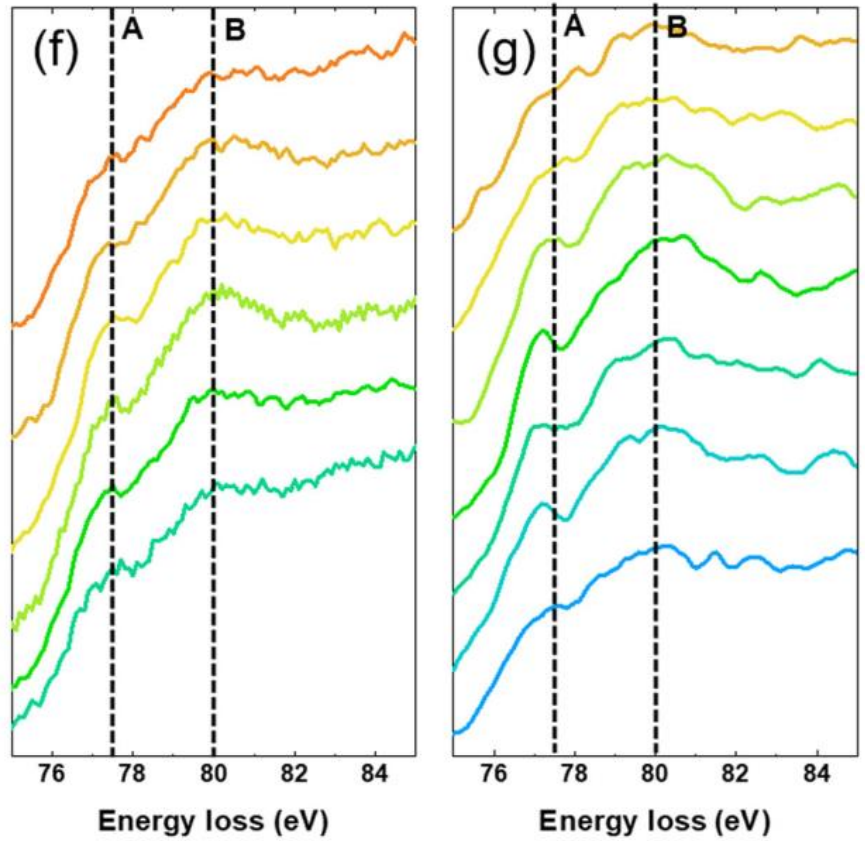

Tunability of Qubit frequency

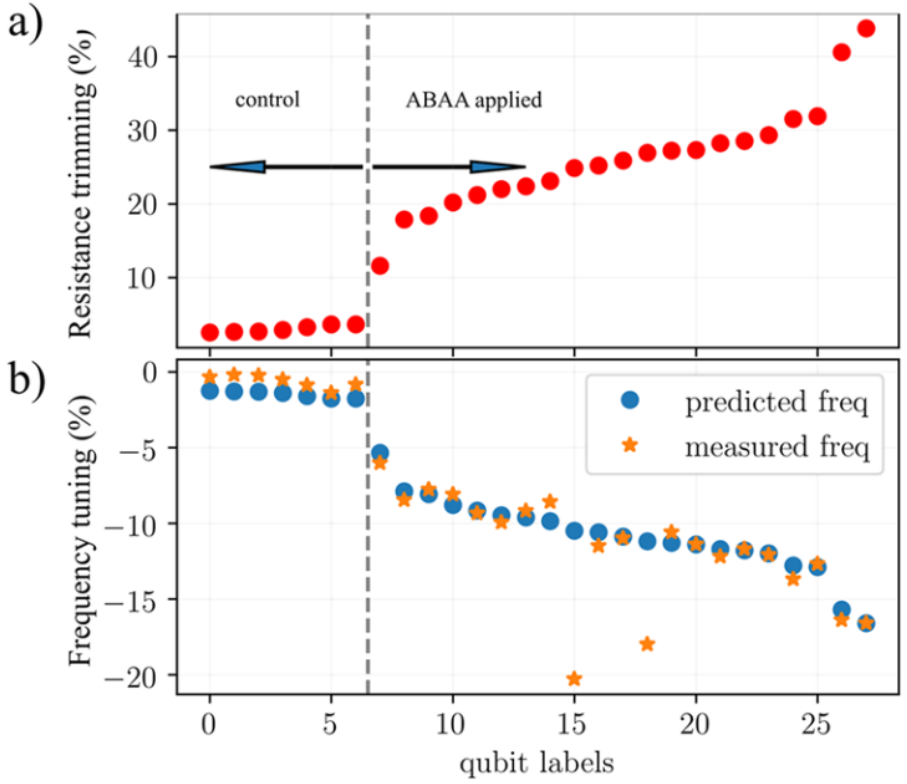

$$I_c = \frac{\pi\Delta}{2eR_n} \qquad E_J = \frac{\hbar}{2e}I_c = \frac{\Phi_0}{2\pi}I_c$$

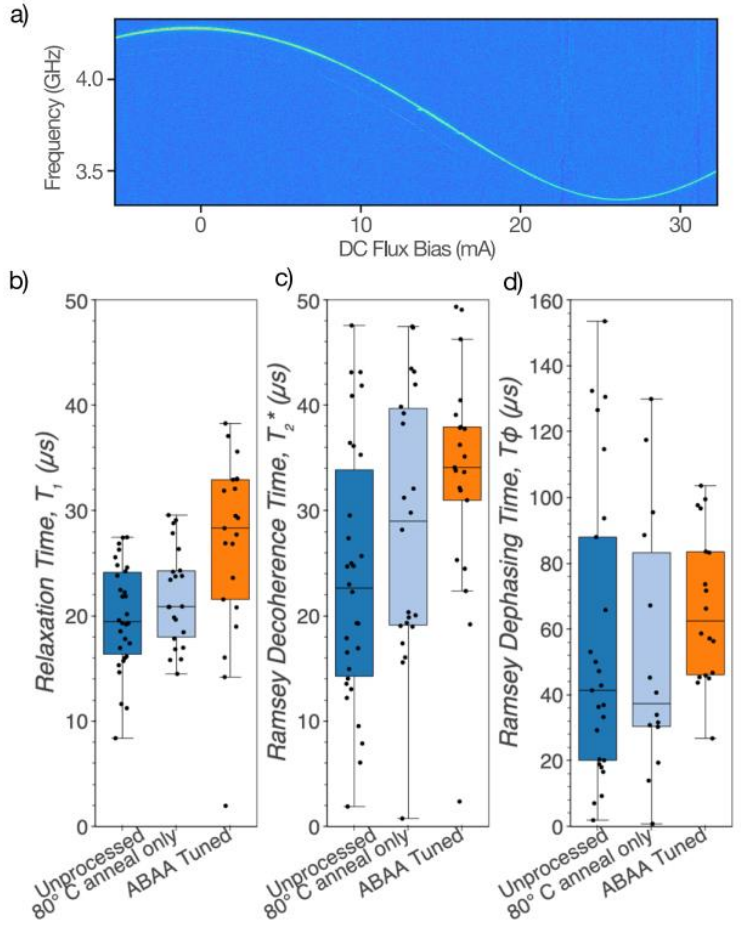

Thanks for your attention

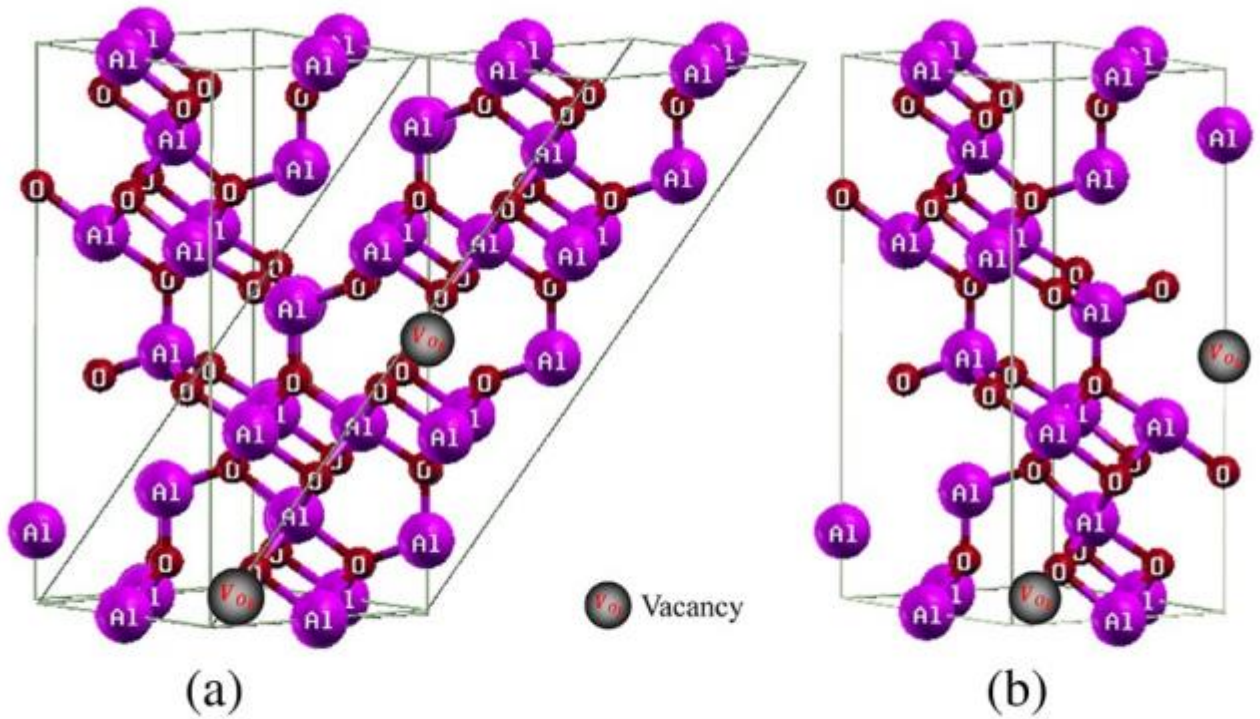

Figure 1 Lattice unit cell conversion. (**a**) Lattice unit cell conversion from triclinic to hexagonal. (**b**) Final γ-Al_2O_3 unit cell which is constructed in this study.

Yazdanmehr et al. Nanoscale Research Letters 2012, 7:488